Published in final edited form as:
Bioconjug Chem. 2010 November 17; 21(11): 2065–2075. doi:10.1021/bc100288c.

Bishydrazide Glycoconjugates for Lectin Recognition and Capture of Bacterial Pathogens

Avijit Kumar Adak[†], **Alexei P. Leonov**[†], **Ning Ding**[‡], **Jyothi Thundimadathil**[§], **Sumith Kularatne**[†], **Philip S. Low**[†], and **Alexander Wei**[*,†]

[†]Department of Chemistry, 560 Oval Drive, Purdue University, West Lafayette, Indiana 47907-2084

Abstract

Bishydrazides are versatile linkers for attaching glycans to substrates for lectin binding and pathogen detection schemes. The α,ω-bishydrazides of carboxymethylated hexaethylene glycol (4) can be conjugated at one end to unprotected oligosaccharides, then attached onto carrier proteins, tethered onto activated carboxyl-terminated surfaces, or functionalized with a photoactive crosslinking agent for lithographic patterning. Glycoconjugates of bishydrazide **4** can also be converted into dithiocarbamates (DTCs) by treatment with CS_2 under mild conditions, for attachment onto gold substrates. The immobilized glycans serve as recognition elements for cell-surface lectins and enable the detection and capture of bacterial pathogens such as *Psuedomonas aeruginosa* by their adsorption onto micropatterned substrates. A detection limit of 10^3 cfu/mL is demonstrated, using a recently introduced method based on optical pattern recognition.

Introduction

Pathogenic microorganisms are an omnipresent threat to global biosecurity, and effective biodetection strategies are necessary to control against the spread of infectious diseases. One viable approach to pathogen detection is to develop diagnostic technologies based on “immutable” recognition of ligands presented on cell surfaces, a vital first step in the cycle of infection. These recognition elements are often low molecular weight molecules such as glycans, which are exploited by pathogens for gaining entry into their host cells. Pathogens must maintain this ligand affinity in order to remain virulent, as those which undergo mutations that disable recognition can no longer infect their target cells. Glycan-based strategies have proven to be particularly successful in detecting bacteria that use lectins for adhesion to host cell membranes (1-8). Furthermore, the immutability of this functional recognition provides an important advantage over antibody-based detection schemes, which are susceptible to nonfunctional mutations that are often irrelevant to pathogen virulence.

Glycoconjugates are also of considerable importance for high-throughput diagnostics or screening of carbohydrate-binding proteins associated with various biological functions or disease states (9-12). Several different covalent chemistries have been successfully implemented for surface functionalization, such as thiol–ene and thiol–maleimide additions

[*]To whom correspondence should be addressed. alexwei@purdue.edu; Tel: (765) 494-5257; Fax: (765) 494-0239.
[‡]Present address: Department of Medicinal Chemistry, School of Pharmacy, Fudan University, Shanghai 201203, P.R. China.
[§]Present address: Peptisyntha, Inc., Torrance, CA 90501.

Supporting Information **Available**. Representative data from flow immunocytometry (Figure S1); control experiments for specificity of pathogen capture (Figures S2–S5); additional immunofluorescence images of lectins bound to DTC-anchored glycan bishydrazides on Au substrate (Figure S6); ^1H and ^{13}C NMR spectra of all new compounds. This material is available free of charge via the Internet at http://pubs.acs.org.

(13-16), Diels-Alder or Cu-catalyzed Huisgen cycloadditions (17-19), nucleophilic addition to epoxides and isothiocyanates (20,21), amide bond ligation (22,23), and Staudinger ligation (24). However, many of these methods require that glycans be in a protected form prior to linker installation, and may involve multiple synthetic or purification steps.

Chemoselective coupling of bifunctional linkers to underivatized glycans is an attractive option, particularly if the reducing-end sugar can be retained in its native cyclized form. Traditional methods involve covalent attachment to the free hemiacetal via reductive amination or glycation, but while the conditions are mild they sacrifice the reducing-end sugar by generating an open-chain structure (25,26). However, weakly basic nucleophiles like aminooxy ethers (H_2NO–R, MeHNO–R) and hydrazides (H_2NNHCO–R) have been shown to condense with hemiacetals in aqueous solutions for efficient glycoconjugation (27-39). Hydrazides have been widely used for bioconjugation onto aldehyde- or carboxyl-presenting surfaces (25); conversely, hydrazides can also be presented on substrates for the specific generation of carbohydrate microarrays.

Here we investigate α,ω-bishydrazides as bifunctional linkers for conjugating underivatized glycans onto various substrates, and present several surface functionalization methods with application toward the binding of lectins and pathogenic bacteria. Bishydrazides can be useful as chelating agents or as supramolecular recognition motifs (40,41), but are most often applied as polymer or biopolymer crosslinking agents (42-44). At first glance, bishydrazides appear to be an unlikely choice for heterofunctionalization, however, we find that they can be selectively monofunctionalized and are versatile linkers for glycoconjugate chemistry.

In this work we use glycan–bishydrazide conjugates to target specific lectins and adhesins found in *Pseudomonas aeruginosa*, an opportunistic, Gram-negative bacteria often found in hospital settings. Nosocomial *Pseudomonas* infections have become increasingly drug-resistant and can be especially pernicious in immunocompromised patients or those suffering from cystic fibrosis, so there is a strong need to develop detection platforms against this pathogen. Epidemiological studies suggest that the risk of *Pseudomonas* infections in healthy individuals increases with environmental pathogen counts above 10^3 cfu/mL (45,46). We aim to address this important public health concern by focusing on glycan recognition as a mechanism for detecting virulent pathogens such as *Pseudomonas* at densities as low as 10^3 cfu/mL, the estimated threshold for nosocomial infection.

Experimental Procedures

General procedures

All starting materials and reagents were obtained from commercial sources, and used as received unless otherwise noted. Fuc(α1→1)Gal(β1→4)Glc (2′-fucosyllactose) was purchased from V-labs, Inc. and GalNAc(β1→4)-Gal(β1→4)Glc (pulmonary trisaccharide **2**) was prepared by multistep synthesis (see below). Bovine serum albumin (BSA), galactose-binding lectin from *Arachis hypogaea* (peanut lectin), anti-lectin rabbit IgG, and FITC-labeled anti-rabbit goat IgG were purchased from Sigma and used as received. *Psuedomonas aeruginosa* (PA01 strain) was obtained from ATCC and grown overnight on agar plates (15 g/L of Bacto Agar, 8 g/mL of Difco Nutrient Broth) at 37 °C. CS_2, CH_2Cl_2, and CH_3CN were freshly distilled from CaH_2 before use; anhydrous and anaerobic MeOH and THF were passed through activated alumina and dipensed from a solvent purification system (MBraun). Reactions were carried out in oven-dried glassware under an inert atmosphere, and solvents were freshly distilled from CaH_2 prior to use. ^1H and ^{13}C NMR spectra were recorded on a Bruker DRX 400 spectrometer operating at 400 MHz and 100 MHz respectively. Chemical shifts (δ) are reported in ppm and referenced to the solvent

used ($CDCl_3$: δ 7.24 and 77.23; CD_3OD: δ 3.31 and 49.15; D_2O: δ 4.80), with coupling constants (*J*) reported in Hz. Deionized water with a resistivity > 18 MΩ·cm was obtained from an ultrafiltration system (Milli-Q, Millipore) and passed through a 0.22-μm filter to remove particulate matter. Silica gel chromatography was performed using ICN SiliTech 32-63 D; reverse-phase HPLC was performed using a Phenomenex Synergi™ C-18 column (250 × 21.2 mm, 4 μM, 80 Å) with UV detection at 214 nm, using an aqueous CH_3CN solvent gradient with a linear flow rate of 10 mL/min.

Neoglycoprotein formation

In a typical experiment, a freshly prepared solution of BSA (10 mg) in phosphate buffered solution (PBS, pH 7.4, 200 μL) was treated with 1-ethyl-3-(3-dimethylaminopropyl)carbodiimide hydrochloride (EDC·HCl, 3 mg in 50 μL PBS) and gently stirred at rt for 1 h. The activated protein solution was then treated with pulmonary trisaccharide–hydrazide conjugate **7** (5.1 mg) in 200 μL PBS, stirred for another 2 h, followed by membrane dialysis and passage through a 0.45-μm filter to remove aggregates and particulate matter. These BSA glycoconjugates could be stored safely at 4 °C for several months.

In situ dithiocarbamate (DTC) and monolayer formation (47,48)

In a typical experiment, a 10 mM solution of lactose–bishydrazide conjugate **6** in deaerated methanol (1.5 mg in 200 μL) was treated with 10 mM solutions of CS_2 (200 μL) and Et_3N (200 μL), then stirred at rt for 1 h in a capped vial prior to use (see below). *In situ* DTC formation was monitored by diluting aliquots of the reaction mixture in deionized water, then measuring increases in characteristic absorption peak intensities at 250 and 292 nm using a Cary-50 spectrophotometer (cell path length = 1 cm).

DTC-anchored monolayers (DAMs) were produced from a freshly prepared solution of **6**–DTC, diluted tenfold with deionized water to a final concentration of 1 mM. A 30-μL aliquot of this stock solution was spread across a lightly oxidized PDMS stamp, then patterned onto Au substrates by microcontact printing (see below). Lactose-terminated DAMs were treated with a solution of peanut lectin (50 μg/mL) and visualized by fluorescence immunostaining. The robustness of the patterned DAMs was evaluated by measuring changes in relative emission intensities over time, with exposure to 2-mercaptoethanol (10 or 100 μM) in PBS. Mean luminosity values and standard deviations were taken from selected regions on the printed substrate using Adobe Photoshop.

UV photolithography

Glass substrates coated with a 50-nm Au layer (1.2 × 1.2 cm^2, Reichert) were cleaned with a piranha solution (2 parts 18 M H_2SO_4, 1 part 30% H_2O_2) for 3 minutes, then thoroughly rinsed with deionized water and dried under a stream of argon. (*Caution*: Piranha solution is a strong oxidizing agent, and should be handled with extreme care). Freshly cleaned substrates were coated with BSA by soaking in a 1 wt% solution in PBS for several hours at rt, followed by immersion in a solution of photoactive glycoconjugate (20 mM in 2:1 MeOH:CH_2Cl_2) for 5 min. The dried films were covered by a quartz photomask having linewidths of 10 or 15 μm and grating periods of 20 μm (Advanced Reproductions Corp.), then exposed to a short-wave ultraviolet lamp (Spectroline, ENF-240C) operating at 254 nm for 25 min, followed by a rinse with MeOH. Microcontact printing (see below) could also be used for patterning photoactive glycoconjugates onto BSA-coated glass slides.

Microcontact printing (μCP)

A freshly prepared poly(dimethylsiloxane) (PDMS) stamp (grating period a = 20 μm; linewidth = 15 μm) was lightly oxidized by a 15-second exposure in a plasma cleaner, then coated with 30 μL of an aqueous solution of **6**–DTC for 2 min (see above for preparation of stock solution). The PDMS stamp was dried in air after blotting excess solution, then pressed lightly onto a roughened Au substrate (see below) at an applied pressure of 6 kPa for 3 seconds, as measured by a mechanical stamper developed in our laboratories. A brass plate was placed at the top of the stamp for even distribution of pressure, and the stamp remained in conformal contact with the substrate for an additional 5 min.

Similar μCP conditions were used to pattern BSA glycoconjugates onto smooth Au substrates. 30 μL of a 1 wt% BSA–lactose hydrazide conjugate (**6**–BSA) in PBS was cast onto a lightly oxidized PDMS stamp as described above, and allowed to sit for 2 min prior to blotting. The PDMS stamp was dried in air, pressed lightly onto the substrate at an applied pressure of 6–12 kPa for 3 seconds, then allowed to remain in conformal contact without added pressure for another 5 min. The micropatterned substrate was washed sequentially with PBS, PBS containing 0.05% Tween-20, then deionized water. The patterned substrate was further incubated with a 5% BSA solution in PBS for 2 h, then washed as above prior to use.

Glycan-directed affinity binding and imaging

Micropatterned glycoconjugates were exposed to either soluble lectins or to live bacterial cultures, and visualized by immunofluorescent staining (bound lectin) or darkfield microscopy (bound bacteria) using an upright microscope (Olympus BH2-RFL-T3) equipped with a darkfield condensor, a high-pressure Hg lamp and filter set for FITC emission, and a DP70 camera for image acquisition. Fluorescence imaging was performed on either glass or on roughened Au substrates; the latter were prepared by immersing clean Au substrates into a solution of $AgNO_3$ (3.7 mM) and hydroquinone (120 mM) in 1.3 M citric acid buffer (pH 3.5) for 1.5 min, followed by a quick rinse with deionized water and immersion in an aqueous $HAuCl_4$ solution (0.5 mM) for 30 min. Roughened Au substrates were dried in air, prior to use.

For affinity patterning with proteins, micropatterned substrates were incubated with a dilute solution of lectin from *Arachis hypogaea* (peanut lectin, 50 μg/mL in PBS) for 2 h at 4 °C. The chip was washed with PBS then treated with a solution of anti-peanut lectin rabbit IgG (1 μg/mL in PBS) for 2 h at 4 °C, then washed again and treated with a solution of FITC-labeled anti-rabbit goat IgG (1 μg/mL in PBS) for another 2 h at 4 °C. The chip was washed with PBS, deionized water, then dried under a stream of air prior to fluorescence imaging.

For affinity patterning with bacteria, *Pseudomonas aeruginosa* (PA01 strain, ATCC) was cultured in NB broth containing choline (0.2% w/v), the latter being necessary for the ectopic expression of fucose-binding lectin PA-IIL (49). Micropatterned substrates were incubated with suspensions of live *Pseudomonas* for 1 h at room temperature, at concentrations ranging from 10^8 to 10^2 cfu/mL. After incubation, the chip was washed with PBS and deionized water prior to darkfield imaging. The density of live *Pseudomonas* was estimated by correlating turbidity measurements (*ca.* 10^9 cfu/mL at O.D. 1) with colony counts obtained by plating serial dilutions. Fluorescent staining of active cultures (SYTO 9/ propidium iodide (PI) stains, Invitrogen) confirmed that >90% of the bacteria were alive prior to their exposure to glycan-patterned substrates.

Darkfield images were subjected to fast Fourier transform (FFT) for pattern demodulation to reveal characteristic peaks in reciprocal lattice space ($k = 1/a$) indicating pathogen capture, according to a recently established protocol (50). Standard sizes and magnification were

established for each micropatterned image, so that the units defining periodicity (in μm) were correctly translated into reciprocal lattice units (in μm^{-1}) in the spectra derived from the FFT images. Signal-to-noise (S/N) levels were determined as the ratio of the peak value at 0.05 μm^{-1} (after background subtraction) to the standard deviation of background intensity; signal qualities were considered acceptable above S/N = 3.

Glycoconjugate–lectin binding immunoassays

Each incubation was performed for 2 hours at rt, followed by rinsing three times with PBS to remove excess proteins prior to the next step. 96-well microtiter plates were coated with **6**–BSA conjugate (10 mg/mL), blocked with a 1% BSA solution to minimize nonspecific protein adsorption, then incubated with increasing concentrations of peanut lectin in the presence or absence of 100-fold excess lactose. Wells were then treated with anti-lectin rabbit IgG (1 μg/mL), followed by anti-rabbit horseradish peroxidase (HRP) IgG (1 μg/mL). The optical absorbances of the wells were analyzed using a microplate reader ($VERSA_{max}$, Molecular Devices) following addition of the HRP substrate (100 μL). Untreated and anti-lectin rabbit IgG treated wells (without primary antibody) in PBS served as negative controls.

For flow cytometry, carboxylic acid functionalized microspheres were conjugated to lactose–bishydrazide **6** via standard EDC coupling for 16 h at rt, followed by multiple washes with PBS. The lactose-conjugated microspheres were dispersed in PBS (1.2 mL) and split into several Eppendorf tubes, which were incubated with increasing concentrations of peanut lectin in the presence or absence of 100-fold excess lactose. After incubating for 2 h at rt, tubes were rinsed and subjected to sequential incubation with anti-lectin rabbit IgG and anti-rabbit FITC IgG as described above. The microspheres were then analyzed for fluorescent immunolabeling using a flow cytometer (Cytomics F500, Beckman Coulter, 10^4 microspheres/sample). Untreated and anti-lectin rabbit IgG (without primary antibody) treated microspheres in PBS served as negative controls.

Hexa(ethylene glycol)-linked bishydrazide (4)—A solution of hexaethylene glycol (5.0 g, 17.70 mmol) in dry THF (50 mL) at room temperature was treated portionwise with potassium *tert*-butoxide (9.92 g, 88.54 mmol) at rt, then stirred for 30 min. The reaction mixture was treated dropwise with ethyl bromoacetate (20 mL, 170 mmol), then stirred at reflux for 20 h. The reaction mixture was cooled to rt, filtered and concentrated, then purified by silica gel chromatography (EtOAc:hexanes 1:1) to yield pure diethyl ester as a colorless oil (5.5 g, 68%). ^{1}H NMR (400 MHz, $CDCl_3$) δ 4.62 (s, 4H), 4.17 (q, 4H, J = 7.2 Hz), 3.71-3.69 (m, 4H), 3.66-3.63 (m, 8H), 3.61-3.59 (m, 12H), 1.23 (t, 6H, J = 7.2 Hz). ^{13}C NMR (100 MHz, $CDCl_3$) δ 170.01, 167.44, 71.01, 70.85, 70.63, 68.88, 68.36, 61.60, 60.79, 14.16. MS (ESI) calcd for $C_{20}H_{38}O_{11}[M]^+$ *m/z* 454.24; found: *m/z* 454.98.

The hexa(ethylene glycol)-linked diester (1.0 g, 2.2 mmol) was dissolved in MeOH (20 mL) passed through an activated alumina column, and treated with anhydrous hydrazine (0.34 mL, 11.0 mmol). The reaction mixture was stirred at rt for 24 h, then concentrated followed by the azeotropic removal of hydrazine using toluene (3 × 10 mL), and finally dried *in vacuo* to afford a light yellow oil (0.92 g, 98%). The resulting bishydrazide could be used to prepare glycoconjugates without further purification. ^{1}H NMR (400 MHz, $CDCl_3$) δ 8.61 (br s, 2H), 4.06 (s, 4H), 3.74-3.58 (m, 28H). ^{13}C NMR (100 MHz, CD_3OD) δ 173.72, 171.15, 73.66, 72.10, 71.51, 71.44, 71.75, 62.12. MS (ESI) calcd for $C_{16}H_{34}N_4O_9Na$ $[M+Na]^+$ *m/z* 449.44; found: *m/z* 449.02.

Heptanediol-linked bishydrazide (5)—Heptane-1,7-diol (1.1 g, 7.56 mmol) was treated with ethyl bromoacetate (4.35 mL, 37.82 mmol) as described above, followed by workup

and silica gel purification (EtOAc:hexanes 1:2) to yield the pure diester as a colorless oil (0.92 g, 36%). ^{1}H NMR (400 MHz, $CDCl_3$) δ 4.15 (t, 4H, *J* = 6.7 Hz), 3.81 (s, 4H), 3.61 (t, 4H, *J* = 6.1 Hz), 1.63 (quint, 4H, *J* = 6.4 Hz), 1.53 (quint, 4H, *J* = 6.7 Hz), 1.34 (3, 6H), 1.26 (m, 2H). ^{13}C NMR (100 MHz, $CDCl_3$) δ 167.52, 66.54, 63.04, 32.77, 29.10, 28.48, 26.13, 25.87, 25.76.

Anhydrous hydrazine (0.185 mL, 5.91 mmol) was treated with heptanediol-linked diester (0.36 g, 1.18 mmol) in methanol (10 mL), according to the reaction conditions described above. After azeotropic removal of the volatiles using toluene, bishydrazide **5** was obtained as an oil (0.32 g, 92%) and could be used to prepare glycoconjugates without further purification. ^{1}H NMR (400 MHz, CD_3OD) δ 3.40 (t, 4H, *J* = 6.4 Hz), 1.40 (quint, 4H, *J* = 6.6 Hz), 1.25-1.21 (m, 10H). ^{13}C NMR (100 MHz, CD_3OD) δ 173.73, 172.39, 62.94, 33.57, 30.38, 26.90. MS (ESI) calcd for $C_{11}H_{24}N_4O_4$ $[M]^+$ *m/z* 276.17; found 276.76.

Hexa(ethylene glycol)-linked lactose–bishydrazide conjugate (6)—A mixture of lactose (10 mg, 0.029 mmol) and bishydrazide linker **4** (124.6 mg, 0.29 mmol) in NaOAc buffer (1 mL, pH 4.2) was stirred at 70 °C for 2 days. The reaction mixture was evaporated under reduced pressure, then purified by reverse-phase HPLC (1–30% aq CH_3CN gradient over 60 min) to afford **6** as colorless oil (18.9 mg, 86%). ^{1}H NMR (400 MHz, CD_3OD) δ 4.62 (s, 1 H), 4.34 (d, 1 H, *J* = 7.5 Hz), 4.14 (d, 1 H, *J* = 8.6 Hz), 4.09-4.03 (m, 3 H), 3.98 (dd, 1 H, *J* = 4.0, 12.0 Hz), 3.92 (dd, 1 H, *J* = 4.0, 8.0 Hz), 3.84-3.79 (m, 2 H), 3.78-3.74 (m, 2 H), 3.70-3.65 (m, 22 H), 3.59-3.52 (m, 6H), 3.49-3.46 (m, 2 H). ^{13}C NMR (100 MHz, CD_3OD) δ 172.32, 171.81, 105.10, 91.89, 80.45, 77.76, 77.11, 76.63, 74.81, 73.66, 73.53, 72.51, 72.14, 72.07, 71.54, 71.31, 70.75, 70.29, 62.48, 62.21, 62.12. MS (ESI) calcd for $C_{28}H_{54}N_4O_{19}Na$ $[M+Na]^+$ *m/z* 773.32; found: *m/z* 773.37.

Hexa(ethylene glycol)-linked pulmonary trisaccharide–bishydrazide conjugate (7)—This compound was prepared according to the procedure above, starting from pulmonary trisaccharide **2** (32 mg, 0.058 mmol) and bishydrazide linker **4** (60.0 mg, 0.14 mmol). Purification by RP-HPLC (1–30% aq CH_3CN gradient over 60 min) yielded glycoconjugate **7** as a light-yellow oil (32 mg, 58%). ^{1}H NMR (400 MHz, CD_3OD) δ 4.61 (d, 1H, *J* = 8.3 Hz), 4.32 (d, 1H, *J* = 7.6 Hz), 4.14 (d, 1H, *J* = 5.5 Hz), 4.08-3.97 (m, 10H), 3.89-3.47 (m, 36H), 2.05 (s, 3H). ^{13}C NMR (100 MHz, CD_3OD) δ 180.31, 175.05, 105.05, 104.44, 93.98, 78.18, 76.80, 76.23, 75.98, 74.69, 74.14, 73.57, 73.07, 72.60, 71.44, 69.53, 62.61, 61.72, 55.05, 24.15, 23.18. MS (ESI) calcd for $C_{36}H_{67}N_5O_{24}Na$ $[M+Na]^+$ *m/z* 976.40; found: *m/z* 976.18.

Hexa(ethylene glycol)-linked 2′-fucosyllactose–bishydrazide conjugate (8)—This compound was prepared according to the procedure above, starting from commercially available 2′-fucosyllactose (2.5 mg, 5.1 μmol) and bishydrazide linker **4** (21.8 mg, 51 μmol). Purification by RP-HPLC (1–40% aq CH_3CN gradient over 60 min) yielded glycoconjugate **8** as a colorless oil (2.9 mg, 51%). ^{1}H NMR (300 MHz, D_2O) *δ* 5.17 (d, 1H, *J* = 3.1 Hz), 4.38 (d, 1H, *J* = 7.7 Hz), 4.10 (m, 1H), 4.02-3.98 (m, 4H), 3.82 (m, 1H), 3.75-3.71 (m, 2H), 3.67-3.43 (m, 41H), 3.29 (m, 1H), 3.23 (m, 1H), 1.09 (d, 1.7 H, *J* = 6.6 Hz), 1.03 (d, 1.3 H, *J* = 6.6 Hz). MS (ESI) calcd for $C_{34}H_{64}N_4O_{23}Na$ $[M+Na]^+$ *m/z* 919.38; found: *m/z* 919.70.

Heptanediol-linked lactose–bishydrazide conjugate (9)—This compound was similarly prepared as that described above, starting from lactose (50 mg, 0.146 mmol) and 1,7-heptanediol bishydrazide **5** (201 mg, 0.736 mmol). Purification by RP-HPLC (1–50% aq CH_3CN gradient over 45 min) yielded glycoconjugate **9** as a light-yellow oil (54 mg, 62%). ^{1}H NMR (400 MHz, CD_3OD) δ 4.30 (d, 1 H, *J* = 7.6 Hz), (d, 1 H, *J* = 8.2 Hz), (d, 1 H, *J* = 4.4 Hz), 3.97 (s, 2H), 3.83-3.77 (m, 2H), 3.67-3.59 (m, 4H), 3.54-3.45 (m, 4H), 3.41-3.35 (m, 2H), 3.22-3.19 (m, 1H), 1.92-1.69 (m, 14H). ^{13}C NMR (100 MHz, CD_3OD) δ

181.97, 173.86, 103.51, 89.97, 78.93, 76.39, 75.95, 75.52, 73.09, 71.55, 70.84, 69.18, 61.66, 61.01, 60.84, 23.98, 20.65, 20.44, 20.37. MS (ESI) calcd for $C_{23}H_{45}N_4O_{14}$ $[M+H]^+$ *m/z* 601.28; found: *m/z* 601.09.

2-Deoxy-3,4,6-tri-*O*-acetyl-2-trichloroacetamido-β-D-galactopyranosyl-(1→4)-2,4,6-tri-*O*-benzyl-β-D-galactopyranosyl-(1→4)-1,2,3,6-tetra-*O*-benzyl-D-glucopyranose (12)—D-Galactosamine thiophenyl glycoside **10** (51) (43.0 mg, 0.044 mmol) and lactose derivative **11** (52) (36.8 mg, 0.066 mmol) were stirred under argon in dry CH_2Cl_2 (2 mL) for 30 min at rt in the presence of freshly activated, powdered 4A molecular sieves. The reaction mixture was cooled to −70 °C, then treated with *N*-iodosuccinimide (NIS, 17.8 mg, 0.079 mmol) and a catalytic amount of triflic acid (TfOH, 2.0 mg, 0.0132 mmol). The reaction mixture was slowly warmed to 0 °C, then stirred for an additional 4 h at rt. The reaction mixture was then neutralized with a few drops of triethylamine, and filtered over a pad of Celite with rinsing by CH_2Cl_2. The mixture was washed with a 10% Na_2SO_3 solution followed by water, and the aqueous layer was extracted twice with CH_2Cl_2. The organic phases were collected and dried over anhydrous Na_2SO_4 and concentrated then purified by silica gel chromatography (EtOAc:hexanes 2:3) to afford trisaccharide **12** as a yellow oil (52.2 mg, 84%). ^{1}H NMR (400 MHz, $CDCl_3$) δ 7.44-7.25 (m, 35 H, ArH), 6.23 (d, 1 H, *J* = 10 Hz, N*H*), 5.26 (d, 1 H, *J* = 2.8 Hz), 4.97 (d, 2 H, *J* = 12.0 Hz), 4.94 (d, 2 H, *J* = 12.0 Hz), 4.88 (d, 2 H, *J* = 8.0 Hz), 4.85 (d, 2 H, *J* = 8.0 Hz), 4.81 (d, 2 H, *J* = 9.6 Hz), 4.78 (d, 2 H, *J* = 8.0 Hz), 4.71 (d, 2 H, *J* = 8.0 Hz), 4.66 (d, 2 H, *J* = 12.0 Hz), 4.51 (d, 1 H, *J* = 8.0 Hz), 4.49 (d, 1 H, *J* = 8.0 Hz), 4.44 (d, 2 H, *J* = 12.0 Hz), 4.13-3.98 (m, 5 H), 3.90 (dd, 2 H, *J* = 6.0, 11.2 Hz), 3.74-3.67 (m, 2 H), 3.62-3.59 (m, 1 H), 3.56 (d, 2 H, *J* = 9.2 Hz), 3.49 (t, 1 H, *J* = 7.6 Hz), 3.36 (d, 1 H, *J* = 9.6 Hz), 2.09 (s, 3H), 2.03 (s, 3H), 1.99 (s, 3H). ^{13}C NMR (100 MHz, $CDCl_3$) δ 170.49, 170.44, 170.30, 162.00, 139.15, 138.66, 137.84, 137.56, 129.00, 128.88, 128.57, 128.42, 128.30, 128.16, 128.00, 127.94, 127.83, 127.70, 127.59, 102.77, 99.51, 92.53, 82.53, 81.76, 82.53, 81.76, 76.11, 75.43, 75.06, 74.32, 73.88, 71.29, 70.64, 69.95, 68.20, 66.31, 60.87, 53.43, 20.87, 20.78, 20.68. MS (MALDI-TOF) calcd for $C_{75}H_{80}Cl_3NO_{19}Na$ $[M+Na]^+$*m/z* 1426.4287; found: *m/z* 1426.4573.

2-Acetamido-2-deoxy-3,4,6-tri-*O*-acetylβ-D-galactopyranosyl-(1→4)-2,4,6-tri-*O*-benzyl-β-D-galactopyranosyl-(1→4)-1,2,3,6-tetra-*O*-benzyl-D-glucopyranose (13)—A solution of trichloroacetamide **12** (50 mg, 0.036 mmol) in dry benzene (1 mL) was treated with tributyltin hydride (52.4 mg, 0.18 mmol) and 2,2′-azobis(isobutyronitrile) (AIBN, 5.86 mg, 0.036 mmol). The mixture was degassed for 15 min with argon then heated to reflux for 1 h, then cooled to rt and, poured into an aq. solution of $NaHCO_3$, and extracted with CH_2Cl_2. The combined extracts were washed with brine, dried over anhydrous Na_2SO_4, and concentrated under reduced pressure. Purification of the residue by silica gel chromatography (EtOAc:hexanes 1:1) afforded acetamide **13** as a yellow oil (32.5 mg, 70%). ^{1}H NMR (400 MHz, $CDCl_3$) δ 7.53-7.23 (35H, ArH), 5.47 (d, 1H, *J* = 8.9 Hz, N*H*), 5.32 (d, 1H, *J* = 2.7 Hz), 4.97 (d, 1H, *J* = 8.0 Hz), 4.91 (d, 2H, *J* = 11.2 Hz), 4.87 (d, 1H, *J* = 8.6 Hz), 4.82 (d, 2H, *J* = 9.3 Hz), 4.78 (d, 2H, *J* = 10.6 Hz), 4.75 (d, 1H, *J* = 11.2 Hz), 4.65 (d, 2H, *J* = 11.2 Hz), 4.61 (d, 2H, *J* = 8.6 Hz), 4.57 (d, 1H, *J* = 4.0 Hz), 4.49 (d, 1H, *J* = 7.8 Hz), 4.42 (d, 1H, *J* = 10.2 Hz), 4.39 (d, 1H, *J* = 6.4 Hz), 4.34 (d, 1H, *J* = 12.0 Hz), 4.24 (d, 2H, *J* = 12.0 Hz), 4.20 (d, 1H, *J* = 10.6 Hz), 4.07 (dd, 1H, *J* = 5.8, 11.2 Hz), 4.00 (d, 1H, *J* = 4.0 Hz), 3.95 (t, 1H, *J* = 12.0 Hz), 3.84 (t, 1H, *J* = 7.4 Hz), 3.77 (dd, 1H, *J* = 4.0, 10.0 Hz), 3.70 (d, 1H, *J* = 9.8 Hz), 3.65-3.62 (m, 1H), 3.55 (t, 1H, *J* = 8.9 Hz), 3.50 (d, 1H, *J* = 7.5 Hz), 3.46 (d, 1H, *J* = 8.0 Hz), 3.42 (dd, 1H, *J* = 2.6, 8.0 Hz), 3.37-3.32 (m, 2H), 2.19 (s, 3H), 2.01 (s, 3H), 1.95 (s, 3H), 1.60 (s, 3H). ^{13}C NMR (100 MHz, $CDCl_3$) δ 170.72, 170.31, 170.22, 169.91, 138.79, 138.53, 138.40, 138.34, 138.22, 137.44, 137.25, 129.04, 128.94, 128.71, 128.32, 128.19, 127.93, 127.87, 127.73, 127.53, 127.34, 127.07, 103.32, 102.76 (2C), 82.79, 81.95, 80.78, 76.10, 75.58, 75.33, 74.45, 73.51, 73.38, 72.07, 71.19, 70.96,

68.75, 68.31, 66.71, 61.35, 51.01, 23.41, 21.08, 20.87. MS (ESI) 1324.25 $[M+Na]^+$. MS (MALDI-TOF) calcd for $C_{75}H_{83}NO_{19}Na$ $[M+Na]^+$ *m/z* 1324.5456; found: *m/z* 1324.5573.

2-Acetamido-2-deoxy-β-D-galactopyranosyl-(1→4)-β-D-galactopyranosyl-(1→4)-D-glucopyranose (2)—A solution of triacetate **13** (100 mg, 0.076 mmol) in dry methanol (5.0 mL) was treated at rt with a catalytic amount of NaOMe in methanol (1 M, 32 μL). The reaction mixture was stirred for 1 h at rt, then treated with Dowex 50WX8 (H^+) resin (500 mg), filtered, and concentrated to dryness. The partially deprotected trisaccharide was dissolved in MeOH (5 mL) and treated with a catalytic amount of $Pd(OH)_2$ on charcoal (80 mg, 20 % on active carbon), purged with H_2, and stirred under an H_2 atmosphere for 12 h. The catalyst was filtered through a pad of Celite, and the filtrate was concentrated to yield pulmonary trisaccharide **2**, as an off-white solid (38 mg, 90 % over two steps). ^{1}H NMR (400 MHz, CD_3OD) δ 4.61 (dd, 1H, *J* = 2.9, 8.4 Hz), 4.48 (d, 1H, *J* = 7.2 Hz), 4.33 (d, 1H, *J* = 7.7 Hz), 4.00 (d, 1H, *J* = 1.7 Hz), 3.90-3.82 (m, 4H), 3.79-3.75 (m, 2H), 3.71-3.64 (m, 2H), 3.62-3.58 (m, 4H), 3.51-3.46 (m, 4H), 3.42-3.39 (m, 1H), 2.02 (s, 3H). ^{13}C NMR (100 MHz, CD_3OD) δ 175.12, 105.12, 104.43, 99.25, 93.69, 80.93, 78.29, 76.82, 76.49, 76.27, 76.00, 74.68, 74.38, 72.59, 69.91, 62.63, 61.95, 61.62, 55.27, 23.15. MS (ESI) calcd for $C_{20}H_{35}NO_{16}Na$ $[M+Na]^+$ *m/z* 568.47; found: *m/z* 568.11.

Fluorescein-labeled 2′-fucosyllactose bishydrazide conjugate (14)—A solution of glycoconjugate **8** (2.2 mg, 2.4 μmol) and fluorescein isothiocyanate (FITC, 1.14 mg, 2.9 μmol) in anhydrous methanol was treated with *N*,*N*-diisopropylethylamine (1.2 μL, 9.8 μmol) and stirred for 10 h at rt. The reaction mixture was concentrated and the residue was purified by RP-HPLC (1–30% aq CH_3CN gradient over 45 min) to yield FITC conjugate **14** as a greenish-yellow solid (2.1 mg, 67%). ^{1}H NMR (400 MHz, CD_3OD) δ 8.18 (d, 1H, *J* = 8.9 Hz), 7.50 (d, 1H, *J* = 2.0 Hz), 7.36 (d, 1H, *J* = 8.8), 4.21 (br s, 2H), 4.14 (d, 1H, *J* = 9.4 Hz), 4.05 (d, 1H, *J* = 9.3 Hz), 3.79-3.78 (m, 4H), 3.74-3.62 (m, 37H), 3.52-3.50 (m, 2H), 3.45-3.42 (m, 1H), 3.24-3.23 (m, 2H), 3.21-3.17 (m, 2H), 3.12-3.09 (m, 1H), 2.00 (3, 3H). MS (MALDI) calcd for $C_{55}H_{76}N_5O_{28}S$ $[M+H]^+$*m/z* 1290.43; found: *m/z* 1290.27.

Photoactive glycan–bishydrazide conjugates (15–17)—In a typical reaction, a solution of pulmonary trisaccharide–bishydrazide conjugate **7** (11 mg, 11.5 μmol) and *N*-5-azido-2-nitrobenzoyloxy-succinimide (ANB-NOS, 5.3 mg, 17.3 μmol) in anhydrous DMF (1 mL) was treated with *N*,*N*-diisopropylethylamine (2.0 μL, 12.7 μmol) and stirred for 12 h at rt, protected from light. The reaction mixture was concentrated and the residue was purified by RP-HPLC (1–30% aq CH_3CN gradient over 45 min) to afford ANS conjugate **16** as a brown solid (8.4 mg, 63%). ^{1}H NMR (400 MHz, CD_3OD) δ 8.08 (s, 1H), 7.89 (br s, 1H), 7.69 (d, 1H, *J* = 8.0 Hz), 7.41 (d, 1H, *J* = 7.9 Hz), 7.14 (t, 1H, *J* = 7.9 Hz), 6.53-6.51 (m, 3H), 5.20 (s, 1H), 4.53 (s, 1H), 4.43 (d, 1H, *J* = 8.0 Hz), 4.17-4.13 (m, 2H), 4.06-4.05 (m, 2H), 4.03-4.01 (m, 2H), 3.77-3.57 (m, 35H), 3.53-3.48 (m, 4H), 1.16 (d, 1H, *J* = 6.4 Hz), 1.10 (d, 1H, *J* = 7.4 Hz). MS (ESI) calcd for $C_{43}H_{70}N_9O_{27}Na$ $[M+H]^+$ *m/z* 1144.43; found: *m/z* 1144.87.

Results and Discussion

Synthesis and reactivity of bishydrazide glycoconjugates

The preparation of bishydrazide crosslinkers have been previously reported in the literature, but with little detail regarding their purification (53). We found bis(carboxymethyl) esters to be practical intermediates for bishydrazide formation, but hydrazinolysis should be performed under strictly anhydrous conditions to avoid the generation of byproducts during glycoconjugate formation. Bishydrazide linkers **4** and **5** were synthesized from their corresponding α,ω-diols by base-promoted carboxymethylation with ethyl bromoacetate in

THF, followed by treatment with excess hydrazine in anhydrous methanol under an inert atmosphere. The bishydrazides prepared in this manner could be collected in nearly quantitative yields simply by removing all volatiles by azeotropic drying with toluene, then used to generate glycoconjugates without further purification.

Glycan–bishydrazide conjugates were prepared by adapting the conditions reported by Shin and coworkers (Scheme 1) (20,21). After an extensive evaluation of reaction conditions using hexa(ethylene glycol)-linked bishydrazide **4** and commercial-grade lactose, we determined that the highest yields were obtained by treating 1 equiv of glycan in AcOH/NaOAc buffer (pH 4.2) with 10 equiv of bishydrazide linker at 70 °C for 48 hours. The glycoconjugates were readily separated from the excess linker by preparative reverse-phase HPLC using an aqueous CH_3CN gradient. ^{13}C NMR analysis of lactose–bishydrazide conjugate **6** indicated the anomeric carbons to have the expected chemical shifts for *O*,*O*- and *N*,*O*-acetals (δ_c 105.10, and 91.89 ppm respectively), confirming the pyranosidic nature of the reducing-end sugar. ^1H NMR coupling constant analysis indicated that the bishydrazides form β-glycoside linkages, in accord with earlier reports (54-57). It should be noted that the formation of bishydrazide glycoconjugates **7** and **8** is not always complete after 48 hours under these conditions; on the other hand, the formation of glycan dimers is negligible, circumventing the need for heterobifunctional linkers.

Glycan–bishydrazide conjugates **7** and **8** were prepared using GalNAc(β1→4)-Gal(β1→4)Glc (2) and 2′-fucosyllactose (Fuc(α1→1)Gal(β1→4)Glc), with the former obtained through multistep organic synthesis (see below). Trisaccharide **2** is a common substructure in the glycans presented on the epithelial lining of the pulmonary tract, and is a high-affinity ligand for adhesins presented on the pili of virulent *Pseudomonas* (58,59). Fucose-presenting glycans such as 2′-fucosyllactose have been shown to be potent ligands for the lectin PA-II, also expressed by *Pseudomonas* (60,61). These glycans presented us an opportunity to evaluate the bishydrazide glycoconjugate chemistry in the context of bacterial pathogen detection.

Briefly, pulmonary trisaccharide **2** was synthesized by the coupling of *N*-trichloroacetyl-protected GalNAc donor **10** (51) with lactose-derived acceptor **11** (52) and *N*-iodosuccinimide–triflic acid activation conditions, yielding the desired β-glycoside **12** in 86% yield (Scheme 2, see Experimental Section for details). Reductive dechlorination with tributyltin hydride, followed by methanolic deacetylation and global debenzylation, yielded trisaccharide **2** in excellent overall yields.

The glycan–bishydrazide conjugates react readily with standard labeling and bioconjugation reagents. Fluorescent glycoconjugate **14** was generated by treatment of 2′-fucosyllactose–bishydrazide **8** with fluorescein isothiocyanate (FITC), whereas photoreactive glycoconjugates **15**–**17** were produced by coupling bishydrazide-linked glycans **6**–**8** with *N*-(5 azido-2-nitrobenzoyloxy)succinimide (ANB-NOS) (Figure 1). In both of these cases, hydrazide coupling was most efficient in anhydrous polar solvents such as DMF and MeOH, using *N*,*N*-diisopropylethylamine as the base (see Experimental Section for details). Neoglycoproteins could also be formed in phosphate-buffered saline (PBS) solutions at physiological pH using typical EDC coupling conditions (see Experimental Section) (39), and stored at 4 °C for several months.

The hydrazide-terminated glycoconjugates are also amenable to *in situ* dithiocarbamate (DTC) formation, a recently established method for anchoring amine-terminated ligands onto metal surfaces (47,48,62-69). DTCs are conveniently prepared by the addition of nucleophilic amines to CS_2 in polar organic or aqueous media, and exhibit a strong binding affinity for gold and several types of inorganic oxides. Bishydrazide-DTCs can be prepared

in a similar fashion: in this work, an equimolar mixture of lactose–bishydrazide conjugate **6**, CS_2, and Et_3N in methanol resulted in essentially quantitative formation of DTC triethylammonium salt within 1 hour under ambient conditions (**6**–DTC, Figure 2). The reaction time was determined by using UV absorption spectroscopy to monitor hydrazide-DTC formation based on increases in characteristic peak intensities at 250 and 292 nm (70).

Lectin and bacterial binding by bishydrazide glycoconjugates

Bishydrazide glycoconjugates can be directly attached onto surface-active substrates for the selective capture of lectins and subsequent binding immunoassays. For example, lactose–bishydrazide **6** was attached onto NHS-activated latex microspheres in order to measure the binding affinity of peanut lectin by flow immunocytometry (K_d = 50 nM), using a FITC-labeled secondary antibody for fluorescence detection (Figure 3A and Supporting Information, Figure S1). Selective binding was established by a competition assay against 1 mM lactose, which increased K_d by tenfold. However, in some cases the use of carrier proteins such as BSA is more convenient for surface functionalization by simple physisorption. An ELISA of **6**–BSA conjugate indicates its affinity for peanut lectin to be the same as that measured for lactose–conjugated microspheres.

Glycoconjugates can also be covalently tethered onto protein layers and other organic substrates by photocrosslinking, which provides opportunities to create glycan microarrays and micropatterns by photolithography (71-75). Au substrates coated with a monolayer of BSA were immersed in a solution of lactose–bishydrazide–ANB conjugate **15**, then dried in air and exposed to UV irradiation through a photomask. The intermediate nitrenes that are generated upon UV irradiation (76) presumably insert into the amino acid sidechains of the immobilized BSA, resulting in a patterned array of glycans after washing away the unexposed ligands. Incubation with peanut lectin followed by fluorescence immunostaining revealed well-defined line patterns, defined by the photomask features (Figure 4).

A similar approach was used to generate photopatterned arrays of the pulmonary trisaccharide and 2′-fucosyllactose on BSA-coated substrates, using glycan–bishydrazide–ANB conjugates **16** and **17** respectively. These micropatterned substrates were exposed to the opportunistic pathogen *Pseudomonas aeruginosa* at 10^6–10^8 cfu/mL, then washed and imaged by optical darkfield microscopy to visualize patterns of glycan-immobilized bacteria in a label-free manner (Figure 5 and Supporting Information, Figures S2 and S3). Specificity for **16** and **17** was confirmed by introducing *Pseudomonas* to control substrates patterned with lactose–bishydrazide conjugate, which resulted in no apparent binding. Furthermore, only live *Pseudomonas* were captured by the trisaccharide ligands; exposing the bacteria to UV irradiation for 2 hour prior to their introduction resulted again in no observable pattern (Supporting Information, Figure S4). We note that the patterns formed by bacterial adhesion at lower pathogen densities can be well below saturation levels, however our pathogen detection method only requires a fill factor of a few percent for pattern recognition, as will be demonstrated shortly.

Glycan–bishydrazide conjugates could also be patterned onto substrates by microcontact printing (μCP), a well-established “soft lithography” technique based on microfabricated polydimethylsiloxane (PDMS) stamps for the physical transfer of organic or biomolecular ligands, including glycans (77-81). Stamps imprinted with 20-μm gratings were coated with solutions of **7**–BSA or **8**–BSA in phosphate buffer, then dried in air and placed in conformal contact with activated glass slides under lightly applied pressure (see Scheme 3 and Experimental Section). The substrates were blocked then exposed for one hour to *Pseudomonas* at 10^2–10^8 cfu/mL, then evaluated for evidence of patterned pathogen capture (Figure 6). On average, we find the pattern transfer of **7**–BSA by μCP to be more consistent

than that produced by photolithography, and remarkably reliable for mediating bacterial adhesion at low pathogen densities.

Visual inspection of the patterned glycan slides can indicate *Pseudomonas* capture at a concentration of 10^5 cfu/mL (Figure 6D). However, image processing by fast Fourier transform allows the linear array of scattering signals to be analyzed as reciprocal lattice peaks, enabling much lower limits of detection **Error! Reference source not found**. These demodulated signals are largely separated from background noise, and can be presented with much greater contrast than the original darkfield images (Figure 6A–H, *insets*). As a result, we find that slides patterned with **7**–BSA can detect *Pseudomonas* capture in a label-free manner, with acceptable signal-to-noise (S/N) ratios down to 10^3 cfu/mL (Figure 6F).

Interestingly, we observe that our *Pseudomonas* cultures have a much lower avidity for 2′-fucosyllactose **8** than for pulmonary trisaccharide **7**, which are recognized by adhesins that are constitutively presented at the tips of bacterial pili (82). Whereas affinity for **7**–BSA is robust and minimally affected by the presence of competing GalNAc or lactose up to 100 mM (Supporting Information, Figure S5), affinity for **8**–BSA is observed only when the bacteria has been cultured in the presence of choline (49). It has been shown that the expression of the fucose-binding lectin PA-IIL is regulated by quorum sensing circuitry (*las* and *rhl*), which are activated in an environmentally dependent (paracrinal) fashion (83,84).

Presentation of glycan–bishydrazides on metal surfaces by *in situ* dithiocarbamate formation

Biosensor applications are often performed with gold substrates, like those based on surface plasmon resonance (SPR) and quartz crystal microbalance (QCM) (85,86). For short-term biosensing studies, it is often appropriate to employ chemisorptive ligands such as ω-functionalized alkanethiols, which are well known to form self-assembled monolayers (SAMs) on gold surfaces (87). However, alkanethiol-based SAMs can have limited stability when exposed to even mildly oxidizing conditions (88), so it is worth considering other types of chemisorptive ligands that can support robust surface functionalization under variable environments or in physiological settings.

DTC-anchored monolayers (DAMs) are useful alternatives to thiol-based SAMs, as they have been shown to have greater resistance to surface desorption or oxidative degradation (47). Although earlier studies involving *in situ* DTC and DAM formation have been conducted with alkyl- and dialkylamines (47,48,62-69), hydrazide-DTCs can be formed just as easily and may also serve as chemisorptive ligands. Lactose–bishydrazide **6** was thus converted into the corresponding DTC (Figure 2), then diluted in water and deposited onto a PDMS stamp for pattern transfer onto a chemically roughened Au surface by μCP. The patterned substrates were blocked by BSA and incubated with peanut lectin, whose binding to lactose-terminated DAMs was visualized by immunofluorescent staining (Figure 7). It is important to note that Au substrates are often incompatible with fluorescence imaging due to their propensity to quench emission; however, radiative decay rates can be accelerated on roughened Au substrates by coupling with local plasmon modes, and may even produce a net gain in emission (89).

As expected, the oriented presentation of **6**–DTC on Au surfaces is well suited for the immobilization of multivalent lectins, and patterned substrates can be soaked in PBS for extended periods without concern for degradation. To further establish whether glycan–bishydrazide DAMs are capable of providing robust support as carbohydrate microarrays for protein screening or pathogen binding, we investigated their stability in the presence of 2-mercaptoethanol (ME), a polar thiol that is frequently used to displace alkanethiol-based SAMs from Au surfaces (90). This displacement assay is important in the context of

physiological sensing, as biogenic thiols such as cysteine and glutathione can also be considered as competing adsorbates. The immunofluorescent patterns on roughened Au substrates were thus exposed to 10 μM or 100 μM ME in PBS at room temperature for 2 days, with monitoring of selected regions at different exposure times by fluorescence microscopy (Supporting Information, Figure S6). Both conditions produced very gradual decay profiles, with an estimated halflife of over 80 hours (Figure 7B). It should be mentioned that displacement assays with millimolar levels of ME could not be performed in this case, as this was sufficient to cause degradation of the roughened Au substrates themselves. Nevertheless, exposure of **6**–DTC ligands to ME at these levels has minimal detrimental effect on DAM stability, and merits further investigation. A direct comparison between SAMs and DAMs is in progress and will be reported in due course.

Conclusions

α,ω-Bishydrazides are useful and versatile linkers for attaching glycans onto substrates for bacterial pathogen detection and lectin profiling. Unprotected glycans are conjugated straightforwardly to bishydrazides with retention of the native pyranose conformation at the reducing end, and can be further conjugated to amine-reactive substrates, carrier proteins, and to metal surfaces by *in situ* DTC formation. With respect to the latter, glycan–bishydrazide–DTCs form robust attachments to roughened gold substrates and are able to withstand displacement by competing thiols under physiologically relevant conditions. Glycan–bishydrazide conjugates can be subsequently employed in microfabrication schemes involving photolithography or PDMS-based microcontact printing for the facile detection of glycan-binding proteins and pathogens, as demonstrated by the patterned adsorption of peanut lectin and *Pseudomonas*. We anticipate using this methodology to support real-time biosensing applications involving protein biomarker or pathogen detection.

Supplementary Material

Refer to Web version on PubMed Central for supplementary material.

Acknowledgments

The authors gratefully acknowledge financial support from the National Institutes of Health (GM-069862), the National Science Foundation (CHE-0243496), the Department of Defense (W911SR-08-C-0001) administered through the U.S. Army RDECOM (Edgewood Contracting Division), and the Center for Sensing Science and Technology at Purdue University. We thank David Lyvers and Ron Reifenberger for their contributions toward FFT analysis, and Youngsoon Kim and James Newton for helpful discussions and assistance with microcontact printing, bacteria culture and quantitative bacterial cell culture analysis.

References

1. Stevens J, Blixt O, Paulson JC, Wilson IA. Glycan microarray technologies: tools to survey host specificity of influenza viruses. Nat Rev Microbiol. 2006; 4:857–864. [PubMed: 17013397]
2. Wang HF, Gu LR, Lin Y, Lu FS, Meziani MJ, Luo PGJ, Wang W, Cao L, Sun YP. Unique aggregation of anthrax (*Bacillus anthracis*) spores by sugarcoated single-walled carbon nanotubes. J Am Chem Soc. 2006; 128:13364–13365. [PubMed: 17031942]
3. El-Boubbou K, Gruden C, Huang X. Magnetic glyco-nanoparticles: A unique tool for rapid pathogen detection, decontamination, and strain differentiation. J Am Chem Soc. 2007; 129:13392–13393. [PubMed: 17929928]
4. Kale RR, Mukundan H, Price DN, Harris JF, Lewallen DM, Swanson BI, Schmidt GJ, Iyer SS. Detection of intact influenza viruses using biotinylated biantennary *S*-sialosides. J Am Chem Soc. 2008; 130:8169–8171. [PubMed: 18529007]

5. Li-Hong Liu LH, Dietsch H, Schurtenberger P, Yan M. Photoinitiated coupling of unmodified monosaccharides to iron oxide nanoparticles for sensing proteins and bacteria. Bioconjugate Chem. 2009; 20:1349–1355.
6. Disney MD, Seeberger PH. The use of carbohydrate microarrays to study carbohydrate-cell interactions and to detect pathogens. Chem Biol. 2004; 11:1701–1707. [PubMed: 15610854]
7. Ngundi MM, Kulagina NV, Anderson GP, Taitt CR. Nonantibody-based recognition: alternative molecules for detection of pathogens. Exp Rev Proteom. 2006; 3:511–524.
8. Kulkarni AA, Weiss AA, Iyer SS. Glycan-based high-affinity ligands for toxins and pathogen receptors. Med Res Rev. 2010; 30:327–393. [PubMed: 20135686]
9. Wu CY, Liang PH, Wong CH. New development of glycan arrays. Org Biomol Chem. 2009; 7:2247–2254. [PubMed: 19462030]
10. Laurent N, Voglmeir J, Flitsch SL. Glycoarrays - tools for determining protein-carbohydrate interactions and glycoenzyme specificity. Chem Commun. 2008:4400–4412.
11. Park S, Lee MR, Shin I. Carbohydrate microarrays as powerful tools in studies of carbohydrate-mediated biological processes. Chem Commun. 2008; 37:4389–4399.
12. Horlacher T, Seeberger PH. Carbohydrate arrays as tools for research and diagnostics. Chem Soc Rev. 2008; 37:1414–1422. [PubMed: 18568167]
13. Park S, Lee MR, Pyo SJ, Shin I. Carbohydrate chips for studying high-throughput carbohydrate-protein interactions. J Am Chem Soc. 2004; 126:4812–4819. [PubMed: 15080685]
14. Park S, Shin I. Fabrication of carbohydrate chips for studying protein-carbohydrate interactions. Angew Chem Int Ed. 2002; 41:3180–3182.
15. Ratner DM, Adams EW, Disney MD, Seeberger PH. Tools for glycomics: mapping interactions of carbohydrates in biological systems. ChemBioChem. 2004; 5:1375–1383. [PubMed: 15457538]
16. Houseman BT, Gawalt ES, Mrksich M. Maleimide-functionalized self-assembled monolayers for the preparation of peptide and carbohydrate biochips. Langmuir. 2003; 19:1522–1531.
17. Houseman BT, Mrksich M. Carbohydrate arrays for the evaluation of protein binding and enzymatic modification. Chem Biol. 2002; 9:443–454. [PubMed: 11983333]
18. Bryan MC, Fazio F, Lee HK, Huang CY, Chang A, Best MD, Calarese DA, Blixt C, Paulson JC, Burton D, Wilson IA, Wong CH. Covalent display of oligosaccharide arrays in microtiter plates. J Am Chem Soc. 2004; 126:8640–8641. [PubMed: 15250702]
19. Michel O, Ravoo BJ. Carbohydrate microarrays by microcontact “click” chemistry. Langmuir. 2008; 24:12116–12118. [PubMed: 18837529]
20. Lee MR, Shin I. Fabrication of chemical microarrays by efficient immobilization of hydrazide-linked substances on epoxide-coated glass surfaces. Angew Chem Int Ed. 2005; 44:2881–2884.
21. Park S, Shin I. Carbohydrate microarrays for assaying galactosyltransferase activity. Org Lett. 2007; 9:1675–1678. [PubMed: 17394347]
22. Blixt O, Head S, Mondala T, Scanlan C, Huflejt ME, Alvarez R, Bryan MC, Fazio F, Calarese D, Stevens J, Razi N, Stevens DJ, Skehel JJ, van Die I, Burton DR, Wilson IA, Cummings R, Bovin N, Wong CH, Paulson JC. Printed covalent glycan array for ligand profiling of diverse glycan binding proteins. Proc Natl Acad Sci USA. 2004; 101:17033–17038. [PubMed: 15563589]
23. De Paz JL, Noti C, Seeberger PH. Microarrays of synthetic heparin oligosaccharides. J Am Chem Soc. 2006; 128:2766–2767. [PubMed: 16506732]
24. Köhn M, Wacker R, Peters C, Schröder H, Soulère L, Breinbauer R, Niemeyer CM, Waldmann H. Staudinger ligation: a new immobilization strategy for the preparation of small-molecule arrays. Angew Chem Int Ed. 2003; 42:5830–5834.
25. Hermanson, GT. Bioconjugate Techniques. 2nd. Academic Press; San Diego: 2008.
26. Xia BY, Kawar ZS, Ju TZ, Alvarez RA, Sachdev GP, Cummings RD. Versatile fluorescent derivatization of glycans for glycomic analysis. Nat Methods. 2005; 2:845–850. [PubMed: 16278655]
27. Lee MR, Shin I. Facile preparation of carbohydrate microarrays by site-specific, covalent immobilization of unmodified carbohydrates on hydrazide-coated glass slides. Org Lett. 2005; 7:4269–4272. [PubMed: 16146404]

28. Park S, Lee MR, Shin I. Construction of carbohydrate microarrays by using one-step direct immobilizations of diverse unmodified glycans on solid surfaces. Bioconjugate Chem. 2009; 20:155–162.
29. Zhi ZL, Powell AK, Turnbull JE. Fabrication of carbohydrate microarrays on gold surfaces: Direct attachment of nonderivatized oligosaccharides to hydrazide modified self-assembled monolayers. Anal Chem. 2006; 78:4786–4793. [PubMed: 16841896]
30. Bohorov O, Andersson-Sand H, Hoffmann J, Blixt O. Arraying glycomics: a novel bi-functional spacer for one-step microscale derivatization of free reducing glycans. Glycobiology. 2006; 16:21C–27C.
31. Liu Y, Feizi T, Campanerorhodes M, Childs R, Zhang Y, Mulloy B, Evans P, Osborn H, Otto D, Crocker P. Neoglycolipid probes prepared via oxime ligation for microarray analysis of oligosaccharide-protein interactions. Chem Biol. 2007; 14:847–859. [PubMed: 17656321]
32. Chen G, Pohl N. Synthesis of fluorous tags for incorporation of reducing sugars into a quantitative microarray platform. Org Lett. 2008; 10:785–788. [PubMed: 18247626]
33. Cló E, Blixt O, Jensen KJ. Chemoselective reagents for covalent capture and display of glycans in microarrays. Eur J Org Chem. 2010:540–554.
34. Thygesen MB, Sauer J, Jensen KJ. Chemoselective capture of glycans for analysis on gold nanoparticles: carbohydrate oxime tautomers provide functional recognition by proteins. Chem Eur J. 2009; 15:1649–1660.
35. Cervigni SE, Dumy P, Mutter M. Synthesis of glycopeptides and lipopeptides by chemoselective ligation. Angew Chem Int Ed. 1996; 35:1230–1232.
36. Zhao YM, Kent SBH, Chait BT. Rapid, sensitive structure analysis of oligosaccharides. Proc Natl Acad Sci U S A. 1997; 94:1629–1633. [PubMed: 9050829]
37. Zhi ZL, Laurent N, Powell AK, Karamanska R, Fais M, Voglmeir J, Wright A, Blackburn JM, Crocker PR, Russell DA, Flitsch S, Field RA, Turnbull JE. A versatile gold surface approach for fabrication and interrogation of glycoarrays. ChemBioChem. 2008; 9:1568–1575. [PubMed: 18561346]
38. Guillaumie F, Thomas ORT, Jensen KJ. Immobilization of pectin fragments on solid supports: novel coupling by thiazolidine formation. Bioconjugate Chem. 2002; 13:285–294.
39. Lohse A, Martins R, Jørgensen MR, Hindsgaul O. Solid-Phase oligosaccharide tagging (SPOT): validation on glycolipid-derived structures. Angew Chem Int Ed. 2006; 45:4167–4172.
40. Bacchi A, Carcelli M, Pelizzi G, Solinas C, Sorace L. Trinuclear copper(II) complexes of bis(acylhydrazone) ligands. Structural analysis and magnetic properties of a sulfato-bridged hexanuclear dimer. Inorg Chim Acta. 2006; 359:2275–2280.
41. Dydio P, Zieliski T, Jurczak J. Bishydrazide derivatives of isoindoline as simple anion receptors. J Org Chem. 2009; 74:1525–1530. [PubMed: 19173632]
42. Bystrický S, Machová E, Malovíková A, Kogan G. Determination of the cross-linking effect of adipic acid dihydrazide on glycoconjugate preparation. Glycoconjugate J. 1999; 16:691–695.
43. Urmenyi AM, Poot AA, Wessling M, Mulder MHV. Affinity membranes for hormone removal from aqueous solutions. J Membrane Sci. 2005; 259:91–102.
44. Ono T, Fujii S, Nobori T, Lehn JM. Soft-to-hard transformation of the mechanical properties of dynamic covalent polymers through component incorporation. Chem Commun. 2007:46–48.
45. Price D, Ahearn DG. Incidence and persistence of *Pseudomonas aeruginosa* in whirlpools. J Clin Microbiol. 1988; 26:1650–1654. [PubMed: 3141463]
46. Guidelines for safe recreational water environments. Vol. 2: Swimming pools and similar environments. World Health Organization; Geneva: 2006. p. 43-45.
47. Zhao Y, Pérez-Segarra W, Shi Q, Wei A. Dithiocarbamate assembly on gold. J Am Chem Soc. 2005; 127:7328–7329. [PubMed: 15898778]
48. Zhu H, Coleman DM, Dehen CJ, Geisler IM, Zemlyanov D, Chmielewski J, Simpson GJ, Wei A. Assembly of dithiocarbamate-anchored monolayers on gold surfaces in aqueous solutions. Langmuir. 2008; 24:8660–8666. [PubMed: 18616309]
49. Gilboa-Garber, N. *Pseudomonas aeruginosa* lectins. In: Kaplan, NP.; Colowick, NP.; Ginsburg, V., editors. Methods in Enzymology. Vol. 83:Complex Carbohydrates, Part D. Academic Press; San Diego: 1982. p. 378-385.Chapter 32

50. Doorneweerd, DD.; Henne, WA.; Reifenberger, RG.; Low, PS. Langmuir. ASAP; 2010. Selective capture and identification of pathogenic bacteria using an immobilized siderophore.
51. Bélot F, Jacquinet JC. Unexpected stereochemical outcome of activated 4,6-*O*-benzylidene derivatives of the 2-deoxy-2-trichloroacetamido-d-*galacto* series in glycosylation reactions during the synthesis of a chondroitin 6-sulfate trisaccharide methyl glycoside. Carbohydr Res. 2000; 325:95–106.
52. Matsuoka K, Goshu Y, Takezawa Y, Mori T, Sakamoto JI, Yamada A, Onaga T, Koyama T, Hatano K, Snyder PW, Toone EJ, Daiyo Terunuma D. Practical synthesis of fully protected globotriaose and its glycopolymers. Carbohydr Polym. 2007; 69:326–335.
53. Vercruysse KP, Marecak DM, Marecek JF, Prestwich GD. Synthesis and *in vitro* degradation of new polyvalent hydrazide cross-linked hydrogels of hyaluronic acid. Bioconjugate Chem. 1997; 8:686–694.
54. Leteux C, Childs RA, Chai W, Stoll MS, Kogelberg H, Feizi T. Biotinyl-l-3-(2-naphthyl)alanine hydrazide derivatives of *N*-glycans: versatile solid-phase probes for carbohydrate-recognition studies. Glycobiology. 1998; 8:227–236. [PubMed: 9451032]
55. Shinohara Y, Sota H, Gotoh M, Hasebe M, Tosu M, Nakao J, Hasegawa Y. Bifunctional labeling reagent for oligosaccharides to incorporate both chromophore and biotin groups. Anal Chem. 1996; 68:2573–2579. [PubMed: 8694260]
56. Ojala CR, Ostman JM, Ojala WH. The saccharide-hydrazide linkage: molecular and crystal structures of the semicarbazide derivatives of d-glucose, d-galactose, and d-xylose, including a ‘forbidden’ conformation of the galactose derivative. Carbohydr Res. 2002; 337:21–29. [PubMed: 11755908]
57. Flinn NS, Quibell M, Monk TP, Ramjee MK, Urch CJ. A single-step method for the production of sugar hydrazides: intermediates for the chemoselective preparation of glycoconjugates. Bioconjugate Chem. 2005; 16:722–728.
58. Krivan HC, Roberts DD, Ginsburg V. Many pulmonary pathogenic bacteria bind specifically to the carbohydrate sequence GalNAcβ1-4Gal found in some glycolipids. Proc Natl Acad Sci USA. 1988; 85:6157–6161. [PubMed: 3413084]
59. Yu L, Lee KK, Hodges RS, Paranchych W, Irvin RT. Adherence of *Pseudomonas aeruginosa* and *Candida albicans* to glycosphingolipid (Asialo-GM1) receptors is achieved by a conserved receptor-binding domain present on their adhesions. Infect Immun. 1994; 62:5213–5219. [PubMed: 7525482]
60. Mitchell E, Houles C, Sudakevitz D, Wimmerova M, Gautier C, Perez S, Wu AM, Gilboa-Garber M, Imberty A. Structural basis for oligosaccharide-mediated adhesion of *Pseudomonas aeruginosa* in the lungs of cystic fibrosis patients. Nat Struct Biol. 2002; 9:918–921. [PubMed: 12415289]
61. Imberty A, Wimmerova M, Mitchell EP, Gilboa-Garber N. Structures of the lectins from *Pseudomonas aeruginosa*: Insights into the molecular basis for host glycan recognition. Microb Infect. 2004; 6:221–228.
62. Huff TB, Hansen MH, Zhao Y, Cheng JX, Wei A. Controlling the cellular uptake of gold nanorods. Langmuir. 2007; 23:1596–99. [PubMed: 17279633]
63. Huff TB, Tong L, Zhao Y, Hansen MN, Cheng JX, Wei A. Hyperthermic effects of gold nanorods on tumor cells. Nanomedicine. 2007; 2:125–132. [PubMed: 17716198]
64. Zhao Y, Newton JN, Liu J, Wei A. Dithiocarbamate-coated SERS substrates: sensitivity gain by partial surface passivation. Langmuir. 2009; 25:13833–13839. [PubMed: 19685897]
65. Guerrini L, Garcia-Ramos JV, Domingo C, Sanchez-Cortes S. Sensing polycyclic aromatic hydrocarbons with dithiocarbamate-functionalized Ag nanoparticles by surface-enhanced Raman scattering. Anal Chem. 2009; 81:953–960. [PubMed: 19127991]
66. Cao R Jr, Diaz A, Cao R, Otero A, Cea R, RA Maria C, Serra C. Building layer-by-layer a bis(dithiocarbamato)copper(II) complex on Au{111} surfaces. J Am Chem Soc. 2007; 129:6927–6930. [PubMed: 17477526]
67. Park MH, Ofir Y, Samanta B, Rotello VM. Robust and responsive dendrimer–gold nanoparticle nanocomposites via dithiocarbamate crosslinking. Adv Mater. 2009; 21:2323–2325.
68. Patel G, Kumar A, Pal U, Menon S. Potassium ion recognition by facile dithiocarbamate assembly of benzo-15-crown-5–gold nanoparticles. Chem Commun. 2009:1849–1851.

69. Morf P, Raimondi F, Nothofer HG, Schnyder B, Yasuda A, Wessels JM, Jung TA. Dithiocarbamates: functional and versatile linkers for the formation of self-assembled monolayers. Langmuir. 2006; 22:658–663. [PubMed: 16401114]
70. Lee AWM, Chan WH, Chiu CML, Tang KT. Ultraviolet spectrophotometric determination of primary and secondary aliphatic amines by formation of dithiocarbamates. Anal Chim Acta. 1989; 218:157–160.
71. Ito Y. Photoimmobilization for microarrays. Biotechnol Prog. 2006:924–932. [PubMed: 16889364]
72. Carroll GT, Wang DN, Turro NJ, Koberstein JT. Photons to illuminate the universe of sugar diversity through bioarrays. Glycoconjugate J. 2008; 25:5–10.
73. Carroll GT, Wang DN, Turro NJ, Koberstein JT. Photochemical micropatterning of carbohydrates on a surface. Langmuir. 2006; 22:2899–2905. [PubMed: 16519501]
74. Liu LH, Dietsch H, Schurtenberger P, Yan M. Photoinitiated coupling of unmodified monosaccharides to iron oxide nanoparticles for sensing proteins and bacteria. Bioconjugate Chem. 2009; 20:1349–1355.
75. Norberg O, Deng L, Yan M, Ramström O. Photo-Click immobilization of carbohydrates on polymeric surfacess: a quick method to functionalize surfaces for biomolecular recognition studies. Bioconjugate Chem. 2009; 20:2364–2370.
76. Lewis RV, Roberts MF, Dennis EA, Allison WS. Photoactivated heterobifunctional cross-linking reagents which demonstrate the aggregation state of phospholipase A_2. Biochemistry. 1977; 16:5650–5654. [PubMed: 921957]
77. Kumar A, Whitesides GM. Features of gold having micrometer to centimeter dimensions can be formed through a combination of stamping with an elastomeric stamp and an alkanethiol “ink” followed by chemical etching. Appl Phys Lett. 1993; 63:2002–2004.
78. Bernard A, Renault JP, Michel B, Bosshard HR, Delamarche E. Microcontact printing of proteins. Adv Mater. 2000; 12:1067–1070.
79. Inerowicz HD, Howell S, Regnier FE, Reifenberger R. Multiprotein immunoassay arrays fabricated by microcontact printing. Langmuir. 2002; 18:5263–5268.
80. Godula K, Rabuka D, Nam KT, Bertozzi CR. Synthesis and microcontact printing of dual end-functionalized mucin-like glycopolymers for microarray applications. Angew Chem Int Ed. 2009; 48:4973–4976.
81. Wendeln C, Heile A, Arlinghaus HF, Ravoo BJ. Carbohydrate microarrays by microcontact printing. Langmuir. 2010; 26:4933–4940. [PubMed: 20092308]
82. Keizer DW, Slupsky CM, Kalisiak M, Campbell AP, Crumpi MP, Sastry PA, Hazes B, Irvin RT, Sykes BD. Structure of a pilin monomer from *pseudomonas aeruginosa*. J Biol Chem. 2001; 276:24186–24193. [PubMed: 11294863]
83. Winzer K, Falconer C, Garber NC, Diggle SP, Camara M, Williams P. The *Pseudomonas aeruginosa* lectins PA-IL and PA-IIL are controlled by quorum sensing and by RpoS. J Bacteriol. 2000; 182:6401–6411. [PubMed: 11053384]
84. Duan K, Surette MG. Environmental regulation of *Pseudomonas aeruginosa* PAO1 Las and Rhl quorum-sensing systems. J Bacteriol. 2007; 189:4827–4836. [PubMed: 17449617]
85. Homola J. Surface plasmon resonance sensors for detection of chemical and biological species. Chem Rev. 2008; 108:462–493. [PubMed: 18229953]
86. Marx KA. Quartz crystal microbalance: a useful tool for studying thin polymer films and complex biomecolecular systems at the solution-surface interface. Biomacromolecules. 2003; 4:1099–1120. [PubMed: 12959572]
87. Love CJ, Estroff LA, Kriebel JK, Nuzzo RG, Whitesides GM. Self-assembled monolayers of thiolates on metals as a form of nanotechnology. Chem Rev. 2005; 105:1103–1170. [PubMed: 15826011]
88. Flynn NT, Tran TN, Cima MJ, Langer R. Long-term stability of self-assembled monolayers in biological media. Langmuir. 2003; 19:10909–10915.
89. Lakowicz JR. Radiative decay engineering: biophysical and biomedical applications. Anal Biochem. 2001; 298:1–24. [PubMed: 11673890]

90. Castelino K, Kannan B, Majumdar A. Characterization of grafting density and binding efficiency of DNA and proteins on gold surfaces. Langmuir. 2005; 21:1956–1961. [PubMed: 15723495]

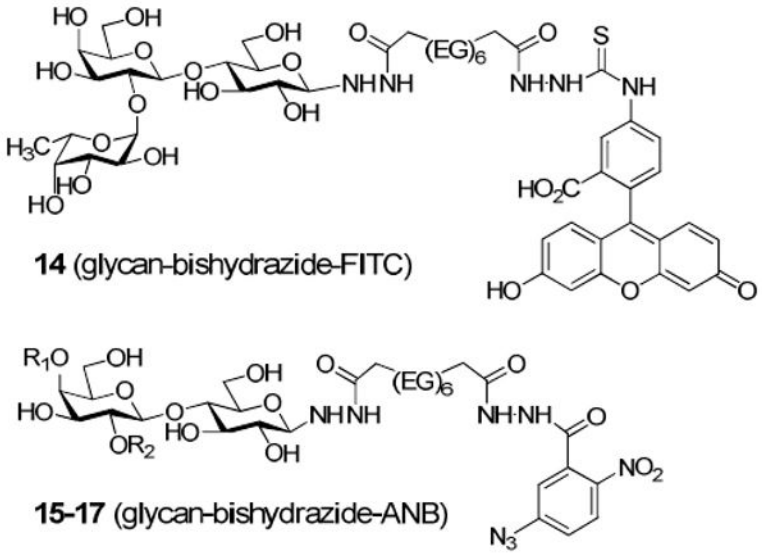

Figure 1.

Glycan–bishydrazide conjugates labeled with fluorescent or photoreactive chromophores. $(EG)_6$ = -$O(CH_2CH_2O)_6$-. **15**: R_1, R_2=H; **16**: R1=β-D-GalNAc, R_2=H; **17**: R_1=H, R_2=α-L-Fuc.

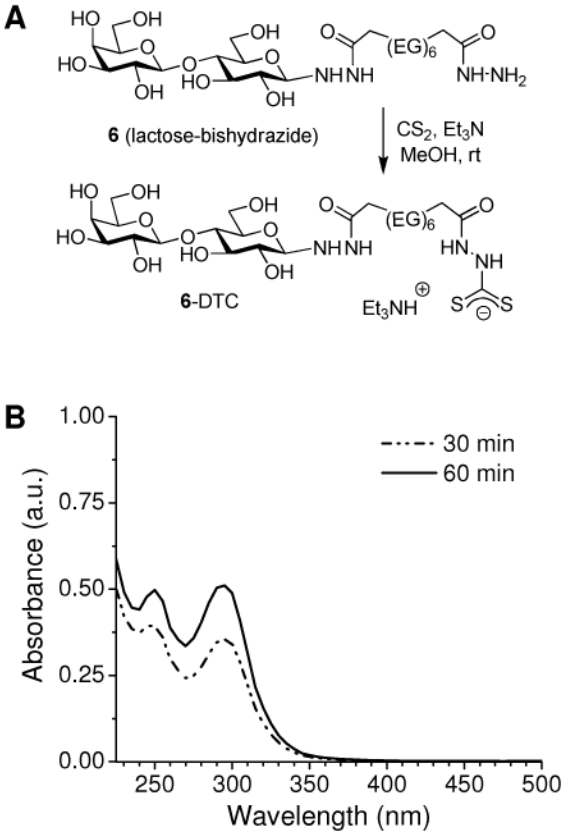

Figure 2.

(A) *In situ* DTC formation starting from lactose–bishydrazide conjugate **6**; $(EG)_6$ = $O(CH_2CH_2O)_6$. (B) UV absorption spectra of **6**–DTC in dilute aqueous solution, taken during *in situ* DTC formation. No further increases in peak intensities were observed after 60 min.

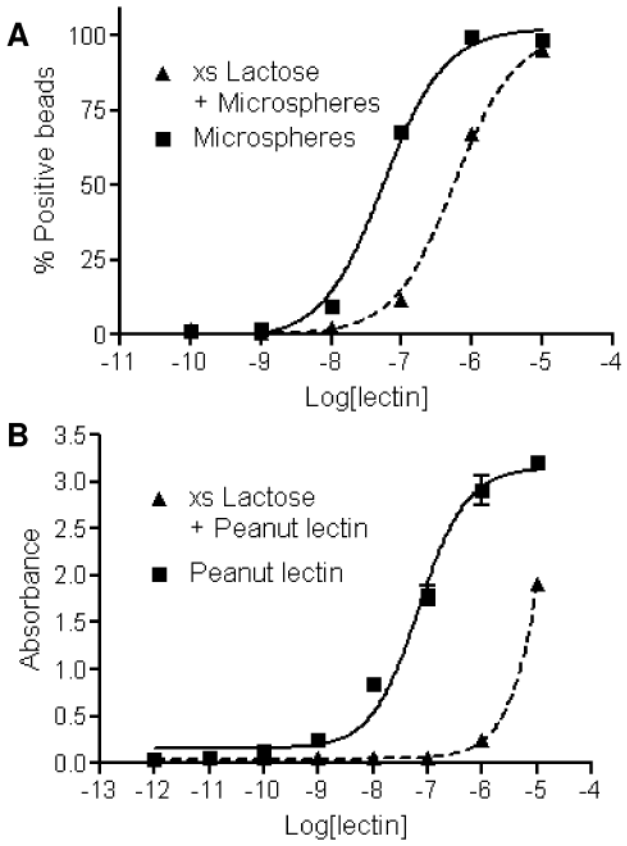

Figure 3.
(A) Affinity and lactose competition assay of peanut lectin binding to microspheres conjugated with lactose–bishydrazide **6** using flow immunocytometry; (B) ELISA and competition assay of peanut lectin binding to immobilized **6**–BSA.

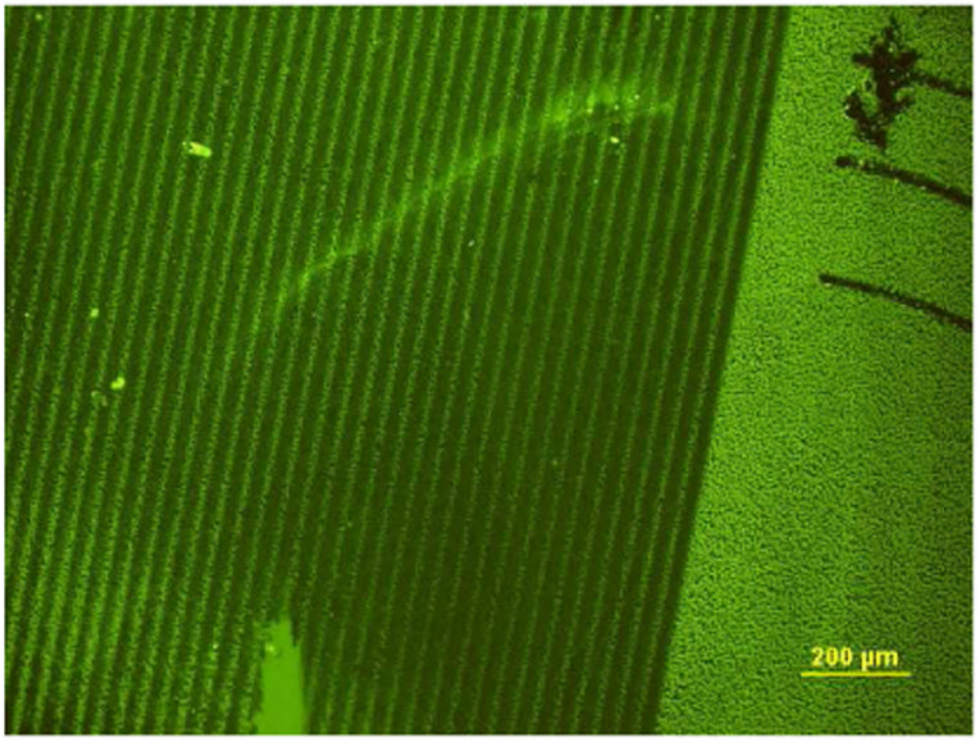

Figure 4.
Fluorescence immunostaining of peanut lectin bound to lactose–bishydrazide–ANB conjugate **15**, photopatterned onto a BSA-coated substrate by UV irradiation (λ=254 nm) through a quartz mask.

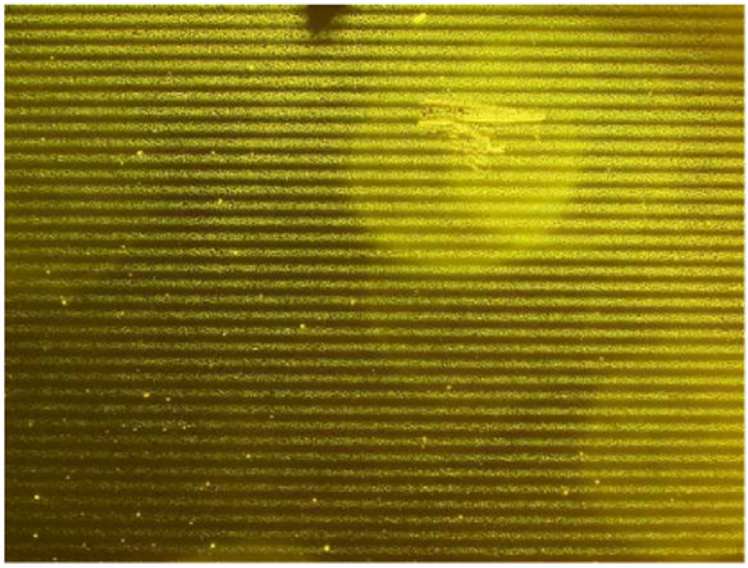

Figure 5.
Capture of *Pseudomonas* on BSA-coated substrates with photopatterned glycan–bishydrazide–ANB conjugate, imaged by darkfield microscopy. Bacterial capture mediated by 2′-fucosyllactose conjugate **17** at 10^8 cfu/mL; grating period a = 20 μm. Additional images in Supporting Information (Figures S2–S4).

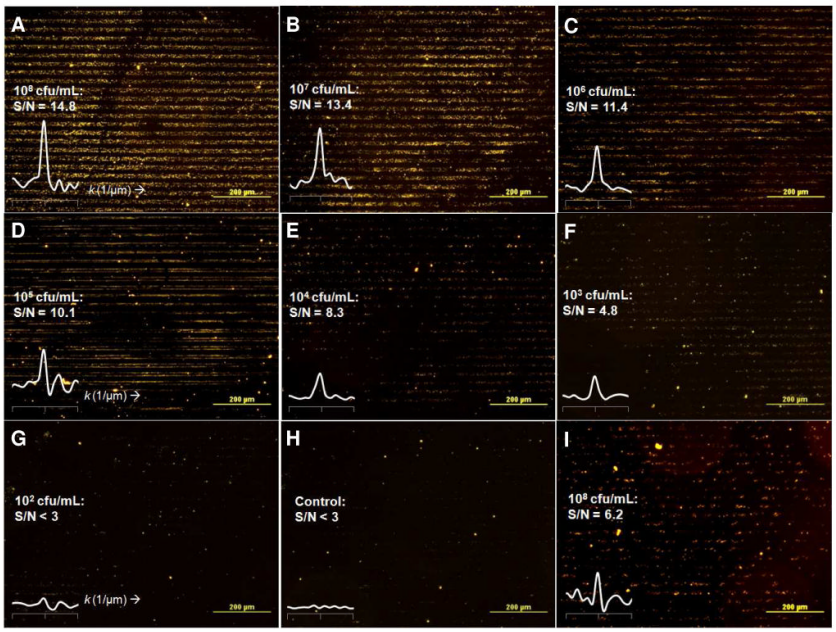

Figure 6.

Capture of live *Pseudomonas* on glass substrates patterned with BSA–glycan bishydrazide conjugates using μCP, as imaged by darkfield microscopy. (A–G) Substrates patterned with pulmonary trisaccharide conjugate **7**–BSA after a 1-hour exposure to *Pseudomonas*, at concentrations ranging from 10^8 to 10^2 cfu/mL. Pattern contrast correlates with signal-to-noise (S/N) ratio defined by reciprocal lattice peak produced by FFT (k=0.05 μm^{-1}). (H) Substrate patterned with **7**–BSA without exposure to bacteria (control). (I) *Pseudomonas* capture mediated by 2′-fucosyllactose conjugate **8**–BSA, in the presence of choline (10^8 cfu/mL).

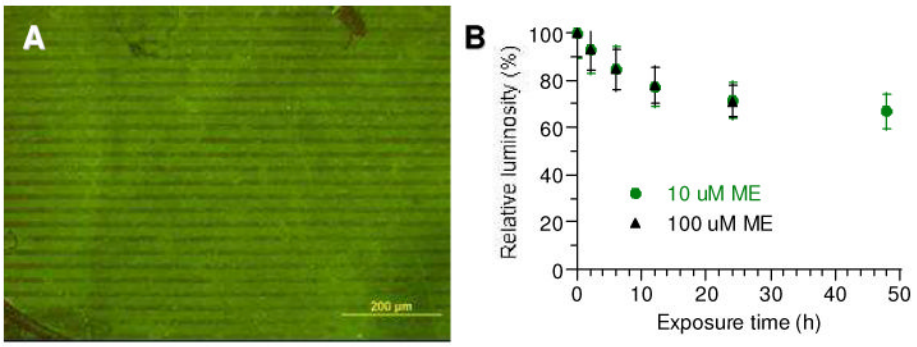

Figure 7.

(A) Fluorescence immunostaining of peanut lectin bound to lactose conjugate **6**–DTC, presented as DAMs on Au substrates by μCP. (B) Stability profile of hydrazide–DTC patterns on roughened Au in PBS containing ME (10 or 100 μM), based on changes in relative luminosity.

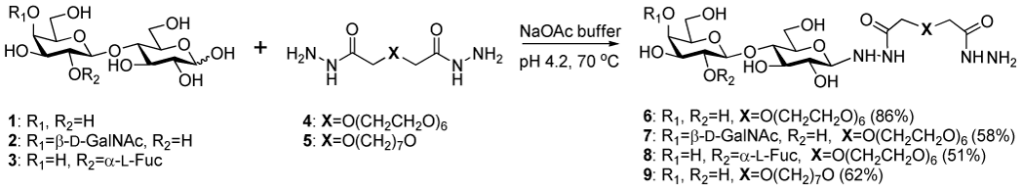

Scheme 1.
Synthesis of glycan–bishydrazide conjugates.

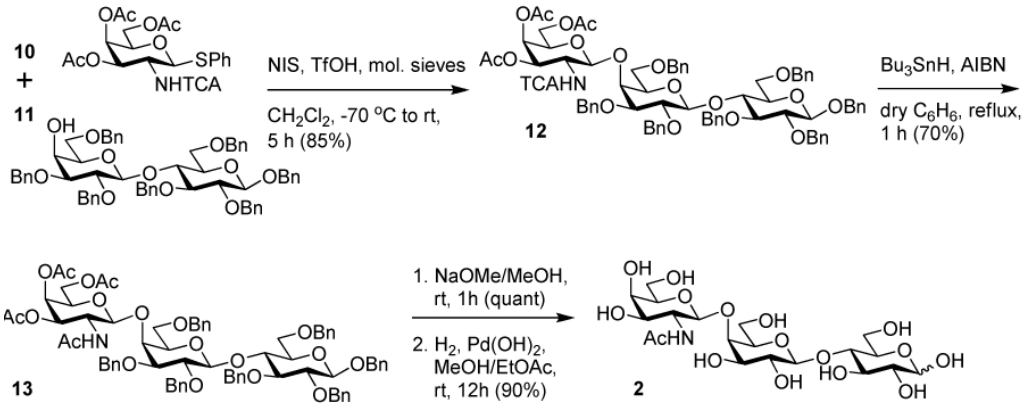

Scheme 2.
Synthesis of pulmonary trisaccharide. TCA = trichloroacetyl.

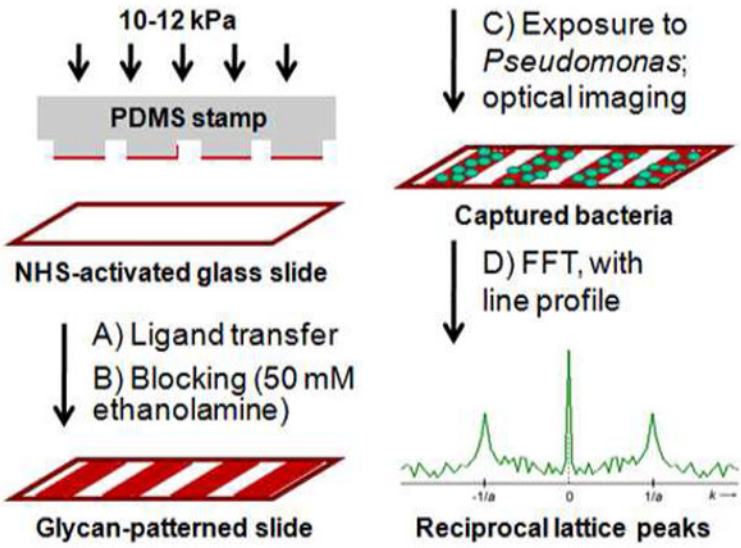

Scheme 3.

(A, B) Glycan-patterned slides by microcontact printing of BSA glycoconjugates onto NHS-activated glass substrates, followed by a blocking step. (C) Patterned capture slides were exposed to *Pseudomonas* at variable concentrations, then imaged under darkfield condtions. (D) Image processing by FFT analysis produced reciprocal lattice peaks at $k=\pm 1/a$ in spectral format; central peak ($k=0$) scales with spatially averaged intensity of original image; noise from nonspecific binding is dispersed throughout k-space.